Design and synthesis of iridium(III) azacrown complex: application as a highly sensitive metal cation phosphorescence sensor

Mei-Lin Ho,[a] Fu-Ming Hwang,[b] Pei-Nung Chen,[b] Ya-Hui Hu,[a] Yi-Ming Cheng,[a] Kung-Shih Chen,[a] Gene-Hsiang Lee,[a] Yun Chi*[b] and Pi-Tai Chou*[a]

Received 22nd August 2005, Accepted 27th October 2005
First published as an Advance Article on the web 18th November 2005
DOI: 10.1039/b511943j

A new metal cation probe **1** bearing a central Ir(III) element and 1-aza-15-crown-5-ether substituted pyridyl pyrazolate as the chelate was synthesized. The octahedral molecular structure of **1** was confirmed using single crystal X-ray diffraction analyses. Subsequent photophysical study showed yellow-green emission at ~560 nm in both fluid solution and solid state at room temperature. Remarkable differentiation in spectral properties upon metal cation (*e.g.* Ca^{2+}) complexation makes complex **1** a highly sensitive phosphorescence probe.

Introduction

Detection of alkali or alkaline earth ions has great potential for practical applications in areas such as analytical chemistry, environmental chemistry and the biological sciences.[1] One method is to use the so-called chemosensor that shows the basic molecular configurations such as chromophore–receptor or chromophore–spacer–receptor. As the receptor can selectively bind with the guest cations, measurable and reversible changes in color and/or luminescence can be detected at the signalling unit (*i.e.* chromophore) linking to the receptor, which allows the recognition and quantification of the metal cation by conventional spectroscopic methods.[2] A common design contains a crown ether to serve as the receptor, together with an organic dye or other metal based fluorophores.[3] Recently, extension was made to systems with third-row transition-metal complexes.[4] Work by a number of groups, mainly pioneered by Schanze and co-workers,[5] has established the importance of utilizing long-lived phosphorescence. Typical signalling involves the switching between non-emissive intra-ligand (^{3}IL) ππ* and metal–to–ligand charge transfer (^{3}MLCT) states,[6] so that a positive luminescent response *vs.* concentration of cation can be obtained. Moreover, it may allow the design of "light-controlled ion switches", for which the cation ejection from the crown ether can be triggered by the effective reduction of electron donation at the receptor on excitation of the nearby chromophore.

In this article, we present a novel system in which an azacrown receptor is attached to the pyridyl pyrazolate chelate of a heteroleptic Ir(III) complex. This design provides three inherent advantages. First, the Ir(III) metal atom forms a highly stable, octahedral coordinated structure and induces strong phosphorescent emission due to the heavy atom effect. Moreover, the ancillary cyclometalated phenyl pyrazole ligands, for which the ππ* energy levels are far higher than those of the respective MLCT and other ligand-centered ππ* excited states,[7] enable both the HOMO and LUMO to reside predominantly on the azacrown substituted pyridyl pyrazolate segment. This architecture enhances the effectiveness of this design over others having more delocalized electronic configurations; the latter should be less capable of recognizing the cation due to the spreading of their electronic perturbation over the whole complex. Thirdly, the azacrown fragment is attached to an anionic pyrazolate chelate ligand, forming a neutral Ir(III) metal complex. Such a charge-neutral characteristic is similar to that of the Re(I) and Pt(II) based sensor complexes, but is in sharp contrast to most of the Ru(II) based polypyridyl sensors,[8] for which the net cationic charge on the overall metal complex is expected to reside, in part, at the azacrown ether site, giving a much reduced sensitivity in recognizing metal cations.[9]

Experimental

General information and materials

Elemental analyses and mass spectra (operating in FAB mode) were carried out at the NSC Regional Instrument Centre at the National Chiao Tung University, Taiwan. ^{1}H and ^{13}C NMR spectra were recorded on a Varian Mercury 400 or an Inova-500 MHz instrument; chemical shifts are quoted with respect to an internal standard, Me_4Si. All synthetic manipulations were performed under a N_2 atmosphere, while solvents were used as received. Synthesis of 1-[4-(1,4,7,10-tetraoxa-13-aza-cyclopentadec-13-yl)-phenyl] ethanone follows the procedures reported by Okahara and co-workers,[10] using the starting materials 4-*N*,*N*-bis(2-hydroxyethyl)aminoacetophenone and triethylene glycol di(*p*-toluenesulfonate). Triethylene glycol di(*p*-toluenesulfonate) was prepared using the literature method,[11] while 1-phenyl-3,5-dimethyl pyrazole (pdpz)H was prepared from the condensation of phenyl hydrazine hydrochloride with acetylacetone according to literature procedures.[12] Treatment of (pdpz)H with $IrCl_3 \cdot nH_2O$ in refluxing methoxyethanol afforded the chloride bridged dimer $[(pdpz)_2IrCl]_2$ in 75% yield;[13] it was then used for subsequent reactions without further purification.

[a]*Department of Chemistry, National Taiwan University, Taipei, 106, Taiwan. E-mail: chop@ntu.edu.tw*
[b]*Department of Chemistry, National Tsing Hua University, Hsinchu, 300, Taiwan. E-mail: ychi@mx.nthu.edu.tw*

Synthesis of [3-(4-aza-15-crown-5-phenyl)pyridyl(1,3-dione)]

To a stirred suspension of NaH (0.75 g, 31.3 mmol) in THF (40 mL), was slowly added 15 mL of THF solution of 1-[4-(1,4,7,10-tetraoxa-13-aza-cyclopentadec-13-yl)-phenyl]-ethanone (2.6 g, 7.8 mmol) at room temperature. The solution was heated to reflux, and ethyl picolinate (2.0 mL, 15 mmol) was added over the course of 1 h. After the addition was completed, the temperature was gradually lowered to room temperature. The solution was continuously stirred for another 3 h and then quenched with dilute HCl solution. After the removal of the solvent, the residue was extracted with CH_2Cl_2 (3 × 60 mL). The extracts were combined, washed twice with water, and dried over anhydrous $MgSO_4$ to afford a yellow solid (2.4 g, 5.4 mmol, 70%).

Selected spectral data. ^{1}H NMR (500 MHz, $CDCl_3$, 294 K): δ 16.87 (s, 1H), 8.69 (d, $J_{HH} = 7.5$ Hz, 1H), 8.13 (d, $J_{HH} = 7.5$ Hz, 1H), 7.98 (d, $J_{HH} = 8.7$ Hz, 2H), 7.87 (dd, $J_{HH} = 7.5$, 4.5 Hz, 1H), 7.49 (s, 1H), 7.42 (dd, $J_{HH} = 7.5$, 4.5 Hz, 1H), 6.68 (d, $J_{HH} = 8.7$ Hz, 2H), 3.77 (t, $J_{HH} = 6.0$ Hz, 4H), 3.67 ~ 3.63 (m, 12H), 3.61 (s, 4H).

Synthesis of 3-(4-aza-15-crown-5-phenyl) pyridyl pyrazole

A solution of [3-(4-aza-15-crown-5-phenyl) pyridyl(1,3-dione)] (1.7 g, 3.8 mmol) and 98% of hydrazine monohydrate (1.94 mL) in 45 mL of anhydrous ethanol was refluxed for 12 h. Next, the solvent was removed under vacuum, and the residue was dissolved in CH_2Cl_2, washed twice with water, dried over anhydrous $MgSO_4$, and the solution was concentrated to dryness. The crude product was purified by silica gel column chromatography (ethyl acetate and methanol = 5 : 1, v/v), giving a light yellow powdery material (azppz)H (1.2 g, 2.74 mmol, 71%).

Selected spectral data. ^{1}H NMR (500 MHz, $CDCl_3$, 294 K): δ 8.6 (d, $J_{HH} = 4.5$ Hz, 1H), 7.79 ~ 7.72 (m, 2H), 7.61 (d, $J_{HH} = 9.0$ Hz, 2H), 7.21 (t, $J_{HH} = 4.5$ Hz, 1H), 6.96 (s, 1H), 6.79 (d, $J_{HH} = 9.0$ Hz, 2H), 3.76 (t, $J_{HH} = 6.2$ Hz, 4H), 3.66 ~ 3.60 (m, 16H).

Preparation of [(pdpz)$_2$Ir(azppz)] (1)

A mixture of $[(pdpz)_2IrCl]_2$ (100 mg, 0.088 mmol), azacrown substituted pyridyl pyrazole (azppzH, 85 mg, 0.19 mmol) and Na_2CO_3 (93 mg, 0.88 mmol) in 2-methoxyethanol (25 mL) was heated to reflux for 4 h. Excess of water was added after cooling the solution to room temperature. The precipitate was collected by filtration and subjected to silica gel column chromatography using ethyl acetate and methanol (5 : 1) as eluent. Yellow-green crystals of [(pdpz)$_2$Ir(azppz)] (**1**) were obtained from repeated recrystallization using a mixture of THF and pentane at room temperature (70 mg, 0.07 mmol, 41%).

Spectral data of 1. MS (FAB, ^{193}Ir) actual *m*/*z* (calculated) [assignment]: 973 (972.4) [M + 1]. ^{1}H NMR (500 MHz, CD_2Cl_2, 294 K): δ 7.68 ~ 7.61 (m, 3H), 7.52 (d, $J_{HH} = 8.5$ Hz, 2H), 7.41 (dd, $J_{HH} = 9.0$, 8.5 Hz, 2H), 6.97 ~ 6.92 (m, 2H), 6.86 (s, 1H), 6.79 (t, $J_{HH} = 6.3$ Hz, 1H), 6.78 ~ 6.71 (m, 2H), 6.58 (d, $J_{HH} = 8.5$ Hz, 2H), 6.42 (d, $J_{HH} = 7.5$ Hz, 1H), 6.31 (d, $J_{HH} = 7.5$ Hz, 1H), 5.98 (s, 1H), 5.94 (s, 1H), 3.68 (t, $J_{HH} = 6.0$ Hz, 4H), 3.60 ~ 3.57 (m, 8H), 3.56 (s, 4H), 3.52 (t, $J_{HH} = 6.0$ Hz, 4H), 2.79 (s, 3H), 2.74 (s, 3H), 1.61 (s, 3H), 1.57 (s, 3H). Anal. calcd. for $C_{46}H_{51}IrN_8O_4$: C, 56.83; H, 5.29; N, 11.53. Found: C, 57.01; H, 5.13; N, 11.73.

Single crystal X-ray diffraction data were acquired on a Bruker Smart CCD diffractometer using λ(Mo K$_a$) radiation (λ = 0.71073 Å). Data collection was executed using the SMART program. Cell refinement and data reduction were made with the SAINT program. The structure was determined using the SHELXTL/PC program and refined using full-matrix least squares. All non-hydrogen atoms were refined anisotropically, whereas hydrogen atoms were placed at the calculated positions and included in the final stage of refinements with fixed parameters. Selected crystal data of **1**: $C_{58}H_{77}IrN_8O_8$, M = 1206.48, triclinic, space group *P*-1, $a = 10.3194(7)$, $b = 16.8549(12)$, $c = 18.3003(13)$ Å, $\alpha = 63.527(2)$, $\beta = 89.840(2)$, $\gamma = 76.006(2)°$, $V = 2744.4(3)$ Å^3, $Z = 2$, $\rho_{calcd} = 1.460$ gcm^{-1}, $F(000) = 1244$, crystal size = 0.35 × 0.17 × 0.08 mm, λ (Mo K$_a$) = 0.7107 Å, $T = 150(1)$ K, $\mu = 2.495$ mm^{-1}, 12566 reflections collected ($R_{int} = 0.0645$), final $R_1[I > 2((I)] = 0.0558$ and wR_2(all data) = 0.1406.

Preparation of [(pdpz)$_2$Ir(dappz)] (2)

A mixture of $[(pdpz)_2IrCl]_2$ (100 mg, 0.088 mmol), NMe_2 substituted pyridyl pyrazole (dappzH, 51 mg, 0.19 mmol) and Na_2CO_3 (93 mg, 0.88 mmol) in 2-methoxyethanol (25 mL) was heated to reflux for 4 h. Excess of water was added after cooling the solution to room temperature. The precipitate was collected by filtration and subjected to silica gel column chromatography using ethyl acetate and methanol (5 : 1) as the eluent. Yellow-green powders of [(pdpz)$_2$Ir(dappz)] (**2**) were collected after washing with acetone; yield: 50 mg, 0.063 mmol, 36%.

Spectral data of 2. MS (FAB, ^{193}Ir): actual *m*/*z* (calculated) [assignment]: 799 (798.3) [M + 1]. ^{1}H NMR (500 MHz, CD_2Cl_2, 294 K): δ 7.68 ~ 7.61 (m, 3H), 7.52 (d, $J_{HH} = 8.5$ Hz, 2H), 7.41 (dd, $J_{HH} = 9.0$, 8.5 Hz, 2H), 6.96 ~ 6.92 (m, 2H), 6.87 (s, 1H), 6.79 (t, $J_{HH} = 6.5$ Hz, 1H), 6.77 ~ 6.71 (m, 2H), 6.66 (d, $J_{HH} = 8.5$ Hz, 2H), 6.42 (d, $J_{HH} = 7.5$ Hz, 1H), 6.31 (d, $J_{HH} = 7.5$ Hz, 1H), 5.98 (s, 1H), 5.94 (s, 1H), 2.89 (s, 6H), 2.79 (s, 3H), 2.74 (s, 3H), 1.62 (s, 3H), 1.57 (s, 3H). Anal. calcd. for $C_{38}H_{37}IrN_8$: C, 57.20; H, 4.67; N, 14.04. Found: C, 57.52; H, 4.43; N, 14.33.

Preparation of [Ph$_2$B(azppz)] (3)

In a 50 mL reaction flask, a mixture of azacrown substituted pyridyl pyrazole (azppzH, 219 mg, 0.5 mmol), 4.4 mL of 2.5 M BPh_3, and 20 mL of anhydrous THF solvent was heated to reflux for 24 h. The solution was then concentrated to dryness and an orange-red crystalline solid of **3** was obtained from recrystallization using a mixture of CH_2Cl_2 and methanol (100 mg, 0.166 mmol, 33%).

Spectral data of 3. MS (FAB, ^{11}B), actual *m*/*z* (calculated) [assignment]: 602 (602.3) [M$^+$]. ^{1}H NMR (500 MHz, CD_2Cl_2, 294 K): δ 8.47 (d, $J = 7.5$ Hz, 1H), 8.08 (m, 1H), 7.84 (d, $J = 7.5$ Hz, 1H), 7.32 (d, $J = 8.5$ Hz, 2H), 7.40 ~ 7.37 (m, 1H), 7.30 ~ 7.28 (m, 4H), 7.24 ~ 7.18 (m, 6H), 6.95 (s, 1H), 6.68 (d, $J = 8.5$ Hz, 2H), 3.72 (t, $J = 6.2$ Hz, 4H), 3.61 ~ 3.60 (m, 8H), 3.58 ~ 3.55 (m, 8H). Anal. calcd. for $C_{36}H_{39}BN_4O_4$: C, 71.76; H, 6.52; N, 9.30. Found: C, 71.40; H, 6.61; N, 9.27.

Measurements

Steady-state absorption and emission spectra were recorded by a Hitachi (U-3310) spectrophotometer and an Edinburgh (FS920) fluorimeter, respectively. Emission quantum yields were measured at excitation wavelength $\lambda_{exc} = 380$ nm in CH_2Cl_2 at room temperature. In this approach, coumarin 480 (Exciton, $\Phi_r = 0.93$ in EtOH) was used as the reference. The association constant K_a of 1 : 1 **1**/guest complex formation calculated by the UV-Vis absorption method is obtained by the following equation.[14]

$$\frac{A_0}{A_0 - A} = \left(\frac{\varepsilon_M}{\varepsilon_M - \varepsilon_p}\right)\left[\frac{1}{K_a C_g} + 1\right] \quad (1)$$

where C_g is the added guest (*e.g.* Ca^{2+}) concentration. A_0 (ε_M) and A (ε_P) denote the absorbance (molar extinction coefficient) of free **1**, and in solution after adding *e.g.* Ca^{2+}, respectively, at a selective wavelength. Eqn. (1) can be further extended to the emission titration experiment expressed as[14]

$$\frac{F_0}{F_0 - F} = \frac{\Phi_M \varepsilon_M}{(\Phi_M \varepsilon_M - \Phi_p \varepsilon_p)}\left(\frac{1}{K_a C_g} + 1\right) \quad (2)$$

where F_0 (Φ_M) and F (Φ_P) denote the photoluminescence (quantum yield) of free **1**, and in solution after adding Ca^{2+}, respectively, at a selective wavelength.

For the phosphorescence lifetime measurements in the microsecond region, a third harmonic of an Nd:YAG laser 355 nm (~8 ns) was used as an excitation source. Emission decay was detected by a photomultiplier tube and averaged over 500 shots using an oscilloscope. Laser energy was reduced to <1 mJ pulse^{-1} to prevent possible photochemical decomposition. For the lifetime measurements of <10 ns, the fundamental train of pulses from a Ti-sapphire oscillator (82 MHz, Spectra Physics) was used to produce second harmonics (375 ~ 425 nm, ~120 fs) as an excitation light source. The signal was detected by a time-correlated single photon counting system (Edinburgh OB 900-L). The system response time was determined to be ~30 ps.

Computational methodology

All calculations were performed with the Gaussian03 package.[15] Geometrical optimization on the electronic ground state was carried out using the hybrid Hartree–Fock/Density functional theory (HF/DFT) method, B3LYP.[16] "Double-ζ" quality basis set consisting of Hay and Wadt's effective core potentials (LANL2DZ)[17] was employed for iridium atom and 6-31G* basis[18] for H, C, and N atoms. A relativistic effective core potential (ECP) replaced the inner core electrons of Ir(III), leaving the outer core ($5s^25p^6$) electrons and the $5d^6$ valence electrons. Time-dependent DFT (TDDFT) calculations were then performed with the same functional and basis set at the optimized geometry to obtain electronic transition energies. Oscillator strengths were deduced from the dipole transition matrix elements (for singlet states only).

Results and discussion

A multi-step synthetic pathway leading to the desired iridium metal complexes is depicted in Scheme 1. First of all, an azacrown substituted pyridyl pyrazole ligand, (azppz)H, was obtained from the condensation reaction of an azacrown substituted acetophenone and ethyl picolinate, followed by treatment with hydrazine monohydrate in ethanol solution (Scheme 1). The subsequent reaction of (azppz)H with the chloride bridged dimer complex $[(pdpz)_2IrCl]_2$ and slight excess of Na_2CO_3 in refluxing methoxyethanol solution afforded the required iridium chelate complex $[(pdpz)_2Ir(azppz)]$ (**1**), where (pdpz)H = 1-phenyl-3,5-dimethyl pyrazole. Moreover, the analogous dimethylamino substituted iridium derivative (**2**) and a BPh_2 substituted complex (**3**) (see Scheme 1) bearing identical azppz pyrazolate ligand were synthesized from reaction with the boron reagent BPh_3, and these then served as the standards for photophysical measurements.

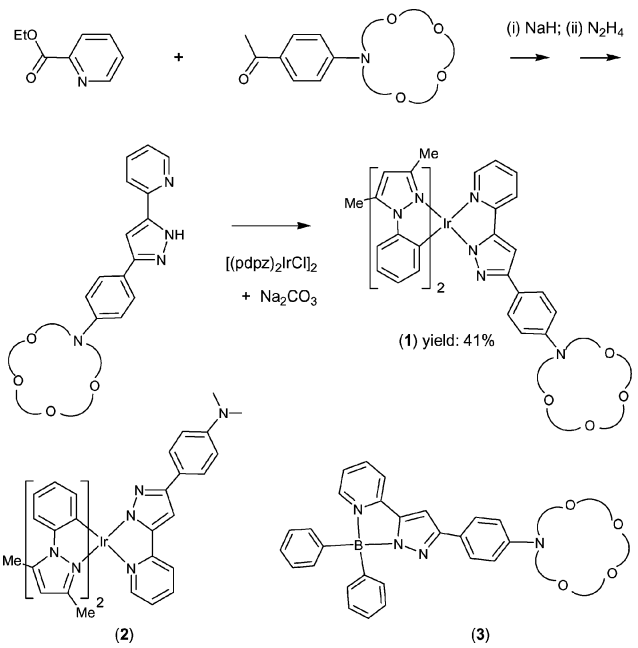

Scheme 1 Synthetic scheme of **1** and molecular structures of **2** and **3**.

As indicated in Fig. 1, single crystal X-ray structural analysis of **1** shows the expected octahedral geometry around the iridium metal center, along with two *N*-phenyl pyrazole fragments and one azacrown substituted pyridyl pyrazolate ligand. The cyclometalated *N*-phenyl pyrazoles adopt an eclipse orientation, while the azacrown pyrazolate chelate is located opposite to the cyclometalated carbon atoms, with the spatial arrangement being akin to those observed for other heteroleptic pyridyl pyrazolate

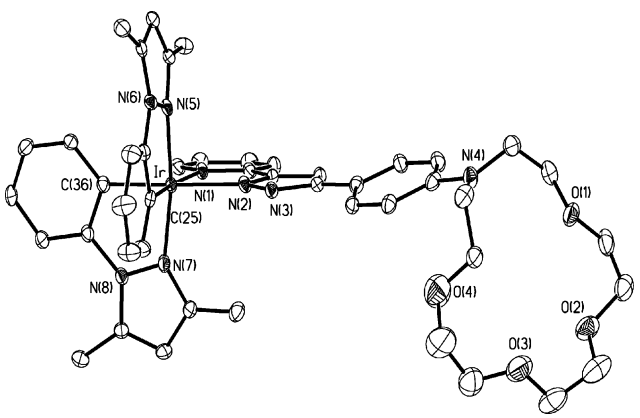

Fig. 1 The X-ray crystal structure of **1**; selected distances: Ir–C(25) = 1.984(6), Ir–C(36) = 2.020(6), Ir–N(1) = 2.155(5), Ir–N(2) = 2.112(5), Ir–N(5) = 2.023(5) and 2.021(5) Å.

complexes.[19] Moreover, the azacrown fragment shows unusually large deformation toward the iridium metal fragment, for which the calculated dihedral angle between the adjacent *p*-phenyl group and the O_4N plane of azacrown is 117.5°.

As shown in Fig. 2, ion-free **1** in CH_3CN exhibits a 318 nm absorption band, accompanied by a shoulder at ~375 nm. In comparison, the boron complex **3** bearing the same pyridyl pyrazolate ligand reveals two low-lying absorption bands with peak wavelengths at 315 and 375 nm, the spectral features of which are similar to that of complex **1**. Due to lack of both MLCT and the transition associated with cyclometalated phenyl pyrazole ligand in boron complex **3**, it is reasonable to assign both 315 and 375 nm bands as the $^1\pi\pi^*$ transitions incorporating pyrazolates → pyridyl types of charge transfer. Transitions associated with MLCT in **1** are probably too weak and thus are hidden inside the $^1\pi\pi^*$ bands. Further firm support is given in the theoretical approaches (*vide infra*). Likewise, absorption features associated with the $^3\pi\pi^*$ intra-ligand bands and ^{3}MLCT could not be resolved although an effective enhancement of the spin–orbit coupling from Ir is expected.

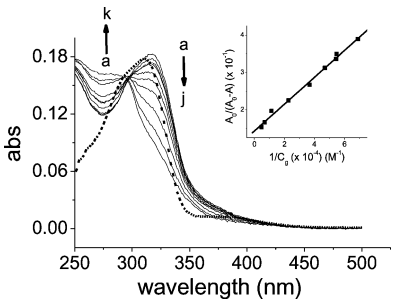

Fig. 2 Absorption spectrum changes of **1** (2.2×10^{-5} M) upon addition of various concentrations of anhydrous $Ca(ClO_4)_2$ in aerated CH_3CN solution (a) 0, (b) 1.45×10^{-5}, (c) 1.83×10^{-5}, (d) 1.84×10^{-5}, (e) 2.13×10^{-5}, (f) 2.71×10^{-5}, (g) 4.39×10^{-5}, (h) 8.70×10^{-5}, (i) 1.45×10^{-4}, (j) 2.03×10^{-4} M. (---) absorption spectrum of **3** in CH_3CN. Insert: the plot of $A_0/A_0 - A$ against $1/[Ca^{2+}]$ at 320 nm.

The emission spectrum of **1** in CH_3CN is depicted in Fig. 3 and the corresponding relaxation dynamics are listed in Table 1. The emission band with a peak wavelength at 560 nm revealed a drastic oxygen quenching effect, the intensity of which decreased from 0.22 in degassed CH_3CN, to ~1.0×10^{-3} upon aeration.

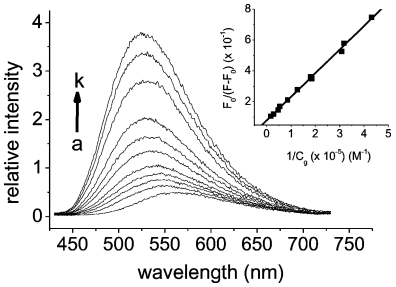

Fig. 3 The emission spectrum changes of **1** (2.2×10^{-5} M) upon addition of various concentrations of anhydrous $Ca(ClO_4)_2$ in aerated CH_3CN solution (a) 0, (b) 3.15×10^{-6}, (c) 3.25×10^{-6}, (d) 5.40×10^{-6}, (e) 5.57×10^{-6}, (f) 7.89×10^{-6}, (g) 1.16×10^{-5}, (h) 2.09×10^{-5}, (i) 3.48×10^{-5}, (j) 5.8×10^{-5}, (k) 1.85×10^{-4} M. λ_{ex}: 300 nm. Insert: the plot of $F_0/F - F_0$ against $1/C_g$ at 520 nm.

Table 1 Photophysical data of **1** and the respective cationic adducts

	PL λ_{max}	*Q.Y.*[a]	lifetime (τ)[a]	K_a
1	560 nm	0.001 (0.22)	38 ns (8.2 μs)	
1/Ca^{2+}	520 nm	0.012 (0.20)	42 ns (0.6 μs)	4.2×10^4
1/Mg^{2+}	518 nm	0.013 (0.23)	48 ns (0.8 μs)	1.6×10^5
1/Ba^{2+}	521 nm	0.010 (0.20)	41 ns (0.6 μs)	5.3×10^3
1/Na^+	520 nm	0.012 (0.18)	40 ns (0.5 μs)	4.7×10^3

[a] data in parentheses are measured in the degassed solution.

Likewise, the corresponding observed lifetime decreased from 8 μs (degassed) to 38 ns (aerated, see Table 1). The ~1/9 diffusion controlled rate of O_2 quenching, in combination with a long radiative decay rate of 3.5×10^4 s^{-1}, leads to an unambiguous conclusion that **1** exhibits predominantly the phosphorescence resulting from the enhancement of Ir(III) spin–orbit coupling.

Upon addition of Ca^{2+}, the absorption and emission titration spectra of **1** (2.2×10^{-5} M) in CH_3CN are shown in Figs. 2 and 3, respectively. Increasing $[Ca^{2+}]$ leads to a hypsochromic shift of the absorption profile, in which the appearance of an isosbestic point at ~295 nm verifies a two-species equilibrium. The 1 : 1 **1**/Ca^{2+} complexation was supported by a straight-line plot for the ratio of absorbance, $A_0/(A_0 - A)$, *versus* $1/[Ca^{2+}]$ (see the experimental section) throughout the titration, and an association constant K_a of 4.0×10^4 M^{-1} was thus deduced in CH_3CN. Likewise, drastic changes on the Ca^{2+} phosphorescence titration spectra were also observed. Upon excitation at the isosbestic point of 295 nm, the 560 nm phosphorescence was gradually blue shifted toward 520 nm, accompanied by the increase of the emission intensity. Taking the emission peak intensity of Ca^{2+}-free and Ca^{2+}-added complex **1** to be F_0 and F, respectively, a straight line plot of $F_0/(F - F_0)$ *versus* $1/[Ca^{2+}]$ (see the experimental section) at *e.g.* 520 nm is depicted in the insert of Fig. 3. The deduced K_a value of 4.2×10^4 M^{-1}, within experimental error, is in agreement with that extracted from the absorption titration.

It should be noted that both complexes **2** and **3** showed negligible changes in their absorption and emission spectra upon addition of Ca^{2+}, manifesting the importance of the coexistence of Ir and 1-aza-15-crown-5-ether in complex **1** toward the Ca^{2+} recognition. The results can be rationalized by weakening the electron donating ability of the aza-nitrogen upon Ca^{2+}/azacrown complex formation and consequently greatly alters the photophysical properties of **1**. This viewpoint can be firmly supported by theoretical modelling. Presently, *ab initio* calculation on **1** is formidable due to its structural complexity. Alternatively, the dimethyl amino analogue **2** was selected, of which the major ligand chromophores remain intact with respect to **1**. Furthermore, the protonated form of **2**, **2H**$^+$, serves as a model for the Ca^{2+} bonded complex **1**. We then applied density functional theory incorporating B3LYP method with 6-31G* basis for non-metal atoms and a relativistic effective core potential for the inner core electrons of Ir(III) metal atom. The resulting frontier orbitals for the low-lying transitions revealed drastic differences between **2** and **2H**$^+$. As shown in Fig. 4, the lowest triplet manifold for **2** exhibits predominantly HOMO → LUMO intraligand charge transfer (ILCT) transition, in which HOMO and LUMO are mainly located at the phenyl pyrazolate and pyridyl chromophores, respectively. In sharp contrast, upon protonation (**2H**$^+$) the

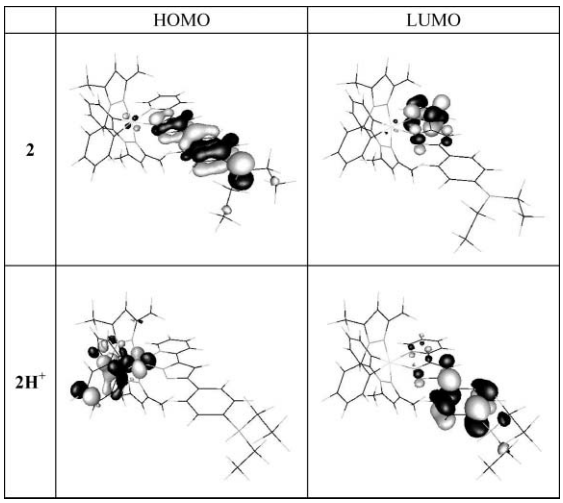

Fig. 4 Frontier orbitals of complexes **2** and **2H**$^+$, see text for detail description.

transition switches greatly to a ligand–ligand charge transfer (LLCT) incorporating cyclometalated phenyl pyrazole ligand (HOMO) → *p*-dialkylamino-phenyl pyrazolate (LUMO). Assuming that the differences in photophysical behavior between **2** and **2H**$^+$ can be likewise applied to **1** and **1**/Ca^{2+} complex, changes of absorption and emission spectra during Ca^{2+} titration are thus be rationalized by the swap of lowest transition from ILCT (*p*-dialkylaminophenyl pyrazolate → pyridine) in **1** to LLCT (cyclometalated phenyl pyrazolate → *p*-dialkylaminophenyl pyrazolate) in **1**/Ca^{2+} complex.

Similar titration experiments have been performed for the hard, bivalent metal cation such as Mg^{2+} and Ba^{2+} and K_a values of 1.6×10^5 M^{-1} and 5.3×10^3 M^{-1}, respectively, were obtained. In another approach, negligible changes of absorption spectra were observed for soft divalent ions like Hg^{2+}. Titration experiments were also performed for Na^+ and the results indicated a K_a value of 4.7×10^3 M^{-1} for the **1**/Na^+ complex formation. The resulting metal ion dependent association strengths can be qualitatively rationalized by the amount of charge density, ρ, specified as $\rho = g/(4/3\pi r^3)$ where g and r are the corresponding formal charge (+1 or +2) and radius, respectively. Evidently, the value of $\rho(Mg^{2+} \sim 0.75$, $Ca^{2+} \sim 0.24$, $Na^+ \sim 0.10$ and $Ba^{2+} \sim 0.13)$[20] correlates well with the trend of K_a values deduced experimentally (see Table 1). Furthermore, negligible spectral changes were observed for K^+ throughout [K^+] of 10^{-2} M. This result can simply be rationalized by the mismatched sizes between K^+ and the 1-aza-15-crown-5 ether.

In solid form **1** exhibits a 565 nm phosphorescent emission with a quantum yield as high as 0.25 ($\tau_p \sim 12$ μs). Thus, from the viewpoint of application, we have also examined whether a similar recognition capability can be applied in the heterogeneous solid film in aqueous solution. Note that **1** is insoluble in water. To simplify the process, a silica-based TLC plate was used as a solid support to soak **1** in CH_3CN so that a complex **1** coated TLC plate was prepared with an optical density of ~1.0 at 350 nm. This plate was then dipped into an aqueous solution (pH ~ 7.0) containing $\sim 10^{-3}$ M $CaClO_4$ for ~30 s, and then vacuum-dried to remove water. With the use of a commercially available UV-lamp (366 nm) as an excitation source, a photograph in TOC demonstrates a salient change of emission from yellow-orange for the Ca^{2+}-free, complex **1** coated TLC plate to a bright green emission upon complexation with the Ca^{2+} ion.

Conclusions

In conclusion, we demonstrate a novel metal ion sensor, complex **1**, based on the rare metal-ion sensitive phosphorescence. In this case, the chromophores designed act as both recognition and signal-transducing units, while the center heavy metal, *i.e.* Ir(III), serves as a perturbing base to enhance the phosphorescence. Thus, the current system is versatile in that functional derivatization can be achieved with methods similar to those strategically designed for the singlet ππ* (*i.e.* fluorescence) ligand chromophores. In view of drastic oxygen quenching, in a steady state approach, one can then saturate the solution with N_2 so that the enhanced phosphorescence can also serve as an additional signalling to distinguish it from the fluorescence interference. Alternatively, in a time-resolved manner, due to its much longer lifetime (even in the aerated solution) than that of typical fluorescence, the associated phosphorescence can be obtained free from fluorescence interferences in the solution simply by acquiring the phosphorescence only after a certain time delay of the excitation pulse. The success in the recognition of Ca^{2+}(aq) in the TLC plate demonstrates its suitability for the future development of a practical device, such as a metal ion sensor anchored on cellular membranes. We thus believe that results presented in this study may spark a broad range of interest in both fundamental approach and applications relevant to the third-row transition metal complexes.

Acknowledgements

This work was funded by the National Science Council of Taiwan, R.O.C. under grants: NSC 93-2113-M-007-012 and NSC 93-2752-M-002-002-PAE. We are also grateful to the National Center for High-Performance Computing for generous amounts of computing time.

References

1 (*a*) H.-G. Löhr and F. Vögtle, *Acc. Chem. Res.*, 1985, **18**, 65; (*b*) W.-S. Xia, R. H. Schmehl and C.-J. Li, *J. Am. Chem. Soc.*, 1999, **121**, 5599; (*c*) B. Valeur and I. Leray, *Coord. Chem. Rev.*, 2000, **205**, 3; (*d*) A. P. de Silva, D. B. Fox, A. J. M. Huxley and T. S. Moody, *Coord. Chem. Rev.*, 2000, **205**, 41; (*e*) A. P. de Silva, D. B. Fox, T. S. Moody and S. M. Weir, *Pure Appl. Chem.*, 2001, **73**, 503.

2 (*a*) K. S. Schanze, D. B. MacQueen, T. A. Perkins and L. A. Cabana, *Coord. Chem. Rev.*, 1993, **122**, 63; (*b*) G. W. Gokel, W. M. Leevy and M. E. Weber, *Chem. Rev.*, 2004, **104**, 2723; (*c*) S.-W. Lai and C.-M. Che, *Top. Curr. Chem.*, 2004, **241**, 27.

3 (*a*) A. P. de Silva, H. Q. Nimal Gunaratne, T. Gunnlaugsson, A. J. M. Huxley, C. P. McCoy, J. T. Rademacher and T. E. Rice, *Chem. Rev.*, 1997, **97**, 1515; (*b*) P. D. Beer and E. J. Hayes, *Coord. Chem. Rev.*, 2003, **240**, 167.

4 (*a*) R. Slone, D. I. Yoon, R. M. Calhoun and J. T. Hupp, *J. Am. Chem. Soc.*, 1995, **117**, 11813; (*b*) Y. Shen and B. P. Sullivan, *Inorg. Chem.*, 1995, **34**, 6235; (*c*) V. W.-W. Yam, C.-L. Chan, C.-K. Li and K. M.-C. Wong, *Coord. Chem. Rev.*, 2001, **216–217**, 173; (*d*) V. W.-W. Yam, R. P.-L. Tang, K. M.-C. Wong, X.-X. Lu, K.-K. Cheung and N. Zhu, *Chem. Eur. J.*, 2002, **8**, 4066; (*e*) L. J. Charbonniere, R. F. Ziessel, C. A. Sams and A. Harriman, *Inorg. Chem.*, 2003, **42**, 3466; (*f*) P. K. M. Siu, S.-W. Lai, W. Lu, N. Zhu and C.-M. Che, *Eur. J. Inorg. Chem.*, 2003, 2749; (*g*) Q.-Z. Yang, L.-Z. Wu, H. Zhang, B. Chen, Z.-X. Wu, L.-P. Zhang and C.-H. Tung, *Inorg. Chem.*, 2004, **43**, 5195.

5 (*a*) D. B. MacQueen and K. S. Schanze, *J. Am. Chem. Soc.*, 1991, **113**, 6108; (*b*) C. E. Whittle, J. A. Weinstein, M. W. George and K. S. Schanze, *Inorg. Chem.*, 2001, **40**, 4053.
6 (*a*) J. F. Michalec, S. A. Bejune, D. G. Cuttell, G. C. Summerton, J. A. Gertenbach, J. S. Field, R. J. Haines and D. R. McMillin, *Inorg. Chem.*, 2001, **40**, 2193; (*b*) J. D. Lewis, L. Bussotti, P. Foggi, R. N. Perutz and J. N. Moore, *J. Phys. Chem. A*, 2002, **106**, 12202; (*c*) J. D. Lewis and J. N. Moore, *Dalton Trans.*, 2004, 1376; (*d*) W.-S. Tang, X.-X. Lu, K. M.-C. Wong and V. W.-W. Yam, *J. Mater. Chem.*, 2005, **15**, 2714.
7 A. B. Tamayo, B. D. Alleyne, P. I. Djurovich, S. Lamansky, I. Tsyba, N. N. Ho, R. Bau and M. E. Thompson, *J. Am. Chem. Soc.*, 2003, **125**, 7377.
8 (*a*) Y. Shen and B. P. Sullivan, *J. Chem. Educ.*, 1997, **74**, 685; (*b*) P. D. Beer, S. W. Dent, N. C. Fletcher and T. J. Wear, *Polyhedron*, 1996, **15**, 2983; (*c*) M. E. Padilla-Tosta, J. M. Lloris, R. Martinez-Manez, M. D. Marcos, M. A. Miranda, T. Pardo, F. Sancenon and J. Soto, *Eur. J. Inorg. Chem.*, 2001, 1475.
9 T. Lazarides, T. A. Miller, J. C. Jeffery, T. K. Ronson, H. Adams and M. D. Ward, *Dalton Trans.*, 2005, 528.
10 H. Maeda, S. Furuyoshi, Y. Nakatsuji and M. Okahara, *Bull. Chem. Soc. Jpn.*, 1983, **56**, 212.
11 Y. Chen and G. L. Baker, *J. Org. Chem.*, 1999, **64**, 6870.
12 K. Y. Lee, J. M. Kim and J. N. Kim, *Tetrahedron Lett.*, 2003, **44**, 6737.
13 (*a*) M. Nonoyama, *J. Organomet. Chem.*, 1975, **86**, 263; (*b*) C.-H. Yang, S.-W. Li, Y. Chi, Y.-M. Cheng, Y.-S. Yeh, P.-T. Chou, G.-H. Lee, C.-H. Wang and C.-F. Shu, *Inorg. Chem.*, 2005, **44**, 7770.
14 (*a*) P.-T. Chou, G.-R. Wu, C.-Y. Wei, C.-C. Cheng, C.-P. Chang and F.-T. Hung, *J. Phys. Chem. B*, 1999, **103**, 10042; (*b*) P.-T. Chou, G.-R. Wu, C.-Y. Wei, C.-C. Cheng, C.-P. Chang and F.-T. Hung, *J. Phys. Chem. B*, 2000, **104**, 7818.
15 M. J. Frisch, G. W. Trucks, H. B. Schlegel, G. E. Scuseria, M. A. Robb, J. R. Cheeseman, J. A. Montgomery, Jr., T. Vreven, K. N. Kudin, J. C. Burant, J. M. Millam, S. S. Iyengar, J. Tomasi, V. Barone, B. Mennucci, M. Cossi, G. Scalmani, N. Rega, G. A. Petersson, H. Nakatsuji, M. Hada, M. Ehara, K. Toyota, R. Fukuda, J. Hasegawa, M. Ishida, T. Nakajima, Y. Honda, O. Kitao, H. Nakai, M. Klene, X. Li, J. E. Knox, H. P. Hratchian, J. B. Cross, V. Bakken, C. Adamo, J. Jaramillo, R. Gomperts, R. E. Stratmann, O. Yazyev, A. J. Austin, R. Cammi, C. Pomelli, J. Ochterski, P. Y. Ayala, K. Morokuma, G. A. Voth, P. Salvador, J. J. Dannenberg, V. G. Zakrzewski, S. Dapprich, A. D. Daniels, M. C. Strain, O. Farkas, D. K. Malick, A. D. Rabuck, K. Raghavachari, J. B. Foresman, J. V. Ortiz, Q. Cui, A. G. Baboul, S. Clifford, J. Cioslowski, B. B. Stefanov, G. Liu, A. Liashenko, P. Piskorz, I. Komaromi, R. L. Martin, D. J. Fox, T. Keith, M. A. Al-Laham, C. Y. Peng, A. Nanayakkara, M. Challacombe, P. M. W. Gill, B. G. Johnson, W. Chen, M. W. Wong, C. Gonzalez and J. A. Pople, *GAUSSIAN 03 (Revision C.02)*, Gaussian, Inc., Wallingford, CT, 2004.
16 (*a*) A. D. Becke, *J. Chem. Phys.*, 1993, **98**, 5648; (*b*) C. Lee, W. Yang and R. G. Parr, *Phys. Rev. B*, 1988, **37**, 785.
17 (*a*) T. H. Dunning and P. J. Hay, In *Modern Theoretical Chemistry*, ed. H. F. Schaefer, III, Plenum Press, New York, 1976, vol. 3, pp. 11; (*b*) P. J. Hay and W. R. Wadt, *J. Chem. Phys.*, 1985, **82**, 270; (*c*) W. R. Wadt and P. J. Hay, *J. Chem. Phys.*, 1985, **82**, 284; (*d*) P. J. Hay and W. R. Wadt, *J. Chem. Phys.*, 1985, **82**, 299.
18 P. C. Hariharan and J. A. Pople, *Mol. Phys.*, 1974, **27**, 209.
19 (*a*) Y.-H. Song, S.-J. Yeh, C.-T. Chen, Y. Chi, C.-S. Liu, J.-K. Yu, Y.-H. Hu, P.-T. Chou, S.-M. Peng and G.-H. Lee, *Adv. Funct. Mater.*, 2004, **14**, 1221; (*b*) F.-M. Hwang, H.-Y. Chen, P.-S. Chen, C.-S. Liu, Y. Chi, C.-F. Shu, F.-I. Wu, P.-T. Chou, S.-M. Peng and G.-H. Lee, *Inorg. Chem.*, 2005, **44**, 1344.
20 Q.-Z. Yang, Q.-X. Tong, L.-Z. Wu, Z. X. Wu, L. P. Zhang and C. H. Tung, *Eur. J. Inorg. Chem.*, 2004, 1948.